

Contents lists available at ScienceDirect

Automatica

journal homepage: www.elsevier.com/locate/automatica



Brief paper

Governor-parameterized barrier function for safe output tracking with locally sensed constraints



Zhichao Li*, Nikolay Atanasov

Department of Electrical and Computer Engineering, University of California San Diego, La Jolla, CA 92093, USA

ARTICLE INFO

Article history:
Received 18 November 2020
Received in revised form 27 October 2022
Accepted 2 March 2023
Available online 29 March 2023

Keywords: Control of constrained systems Tracking Barrier function Reference governor

ABSTRACT

This paper considers output tracking with time-varying constraints, obtained from online sensor measurements, relevant to autonomous system navigation in unknown environments. Inspired by reference governor techniques, we introduce a virtual governor system, whose state specifies an output regulation point for the actual system and is controlled to adaptively track an output reference without violating the constraints. Our main contribution is a governor-parameterized barrier function (PBF) that quantifies the trade-off between safety (distance from constraint violation) and system energy (output-regulation Lyapunov function). The PBF defines a local safe set that varies as the system-governor state or the sensor measurements change. This safe set induces a governor control law, which guarantees safe and stable output tracking for the real system. We demonstrate our adaptive output-tracking controller on a feedback-linearizable system navigating in an unknown environment, where obstacle distances are measured online.

© 2023 Elsevier Ltd. All rights reserved.

1. Introduction

Driven by safety-critical applications in robotics and cyber-physical systems, handling safety constraints simultaneously with system stability has become an important research direction in control theory. Designing provably safe controllers subject to time-varying constraints is a key challenge because often the constraints are only known at execution time. The safety constraints may depend not only on the internal system state but also on the environment and, hence, must be obtained online using sensor measurements.

This paper considers output tracking for a dynamical system with time-varying constraints obtained from online distance measurements to an unsafe set. Our approach is inspired by reference governor techniques (Bemporad, 1998; Kolmanovsky, Garone, & Di Cairano, 2014; Nicotra & Garone, 2018), which enforce safety constraints for a prestabilized system by converting them to constraints on the system's Lyapunov function. The state of a virtual low-order system, called a *governor*, serves as a reference for the actual system and is controlled to ensure that the Lyapunov function constraints remains valid during tracking.

E-mail addresses: zhl355@eng.ucsd.edu (Z. Li), natanasov@eng.ucsd.edu (N. Atanasov).

Most reference governor works, however, have not considered output tracking and assume that the safety constraints are known in advance. Our *contribution* is a governor-parameterized barrier function (PBF), which changes as the governor state, the system state, or the sensor measurements change. The PBF quantifies the trade-off between safety (distance from constraint violation) and system energy (measured by a Lyapunov function), and can be used to regulate the joint governor-system motion to achieve output-tracking with formal safety and stability guarantees.

Related Work. Model predictive control (MPC) (Borrelli, Bemporad, & Morari, 2017; Bravo, Alamo, & Camacho, 2006; Grüne & Pannek, 2017; Mayne, Rawlings, Rao, & Scokaert, 2000) approximates an infinite-horizon optimal control problem with a sequence of finite-horizon problems. With a suitable choice of terminal cost and constraints for the finite-horizon problems, MPC guarantees recursive feasibility and asymptotic stability for linear systems subject to polytopic state and control constraints (Borrelli et al., 2017; Gao, Gray, Tseng, & Borrelli, 2014). There are two main differences between our formulation and MPC techniques. First, we consider an output reference signal which is path-length – but not time-parameterized and track it adaptively based on online sensor measurements. In contrast, standard MPC formulations require a state or output reference model with pre-specified temporal dynamics. Second, we consider a general obstacle set \mathcal{O} and rely on distance measurements at runtime for control synthesis. In contrast, to synthesize a tracking controller, MPC techniques need to approximate the free space using convex regions (Gao, Wu, Lin, & Shen, 2018; Santillo &

We gratefully acknowledge support from United States National Science Foundation RI IIS-2007141. The material in this paper was not presented at any conference. This paper was recommended for publication in revised form by Associate Editor Zongli Lin under the direction of Editor Luca Zaccarian.

^{*} Corresponding author.

Jankovic, 2021). Our approach does not replace MPC but provides another way to deal with non-convex obstacles and reference signals without time parameterization. An MPC controller can be integrated with our approach to synthesize a local output regulation controller (see Section 3 for details) and extend our approach to a broader class of nonlinear systems. We emphasize that in a partially known environment, both our method and MPC-based methods require online estimation of the safety constraints and generation of a reference path in the interior of the safe space and, hence, our method does not guarantee better performance.

Recently, control barrier function (CBF) methods (Ames et al., 2019; Ames, Grizzle, & Tabuada, 2014; Ames, Xu, Grizzle, & Tabuada, 2017) have attracted a lot of attention in safety-critical applications (Ames, Galloway, Sreenath, & Grizzle, 2014; Ames, Grizzle, & Tabuada, 2014; Borrmann, Wang, Ames, & Egerstedt, 2015; Nguyen & Sreenath, 2016; Wu & Sreenath, 2016). Inspired by the seminal work on control Lyapunov functions (CLFs) (Sontag, 1983, 1989), a CBF encodes a safe set implicitly as a superlevel set of a barrier function and provides an elegant way to enforce forward invariance based on the derivative along the system evolution. A key observation (Ames, Grizzle, & Tabuada, 2014) is that the CLF and CBF conditions become linear in the control input for control-affine systems and can be used as constraints in a quadratic programming formulation for safe and stable control synthesis. In the past few years, researchers have advanced this method further, considering robust CBFs for modeling uncertainty and measurement noise (Cosner et al., 2021; Jankovic, 2018). Constructing valid CBFs, however, is known to be challenging (Ames et al., 2019), especially for systems with safety constraints expressed as high-order relative degree CBFs (Nguyen & Sreenath, 2016; Xiao & Belta, 2019). Input constraints, such as boundedness (Breeden & Panagou, 2021; Xu, 2018), smoothness (Ong & Cortés, 2019) and delays (Abel, Janković, & Krstić, 2020), are challenging to handle with CBF techniques. Only a few papers use CBF for safe navigation (Barry, Majumdar, & Tedrake, 2012; Long, Qian, Cortés, & Atanasov, 2021) and often require obstacle information in advance. In contrast, our approach uses local distance measurements and constructs a time-varying barrier function at run time. Note that, to generate a reference path in the interior of the safe set, our approach still requires online obstacle estimation, which may be utilized by an alternative CBF method to similarly guarantee safe control.

Reachability-based methods for safe control rely on precise reachable set approximations. There are many ways to compute reachable sets but funnels (Burridge, Rizzi, & Koditschek, 1999) and Hamilton-Jacobi reachability (Bansal, Chen, Herbert, & Tomlin, 2017; Fisac, Chen, Tomlin, & Sastry, 2015) techniques have been particularly effective in trajectory tracking applications (Herbert et al., 2017; Kousik, Vaskov, Bu, Johnson-Roberson, & Vasudevan, 2020; Majumdar & Tedrake, 2017; Tedrake, Manchester, Tobenkin, & Roberts, 2009). Reachability computations require solving Hamilton-Jacobi partial differential equations (PDE) which is challenging for high-dimensional systems without decomposition methods that split the system into several loworder subsystems (Chen, Herbert, & Tomlin, 2017). A relationship between CBF construction and the value function in Hamilton-Jacobi PDE is established in Choi, Lee, Sreenath, Tomlin, and Herbert (2021) and used to synthesize CBFs with feasibility guarantees under input constraints.

Reference governor techniques (Bemporad, 1998; Kolmanovsky et al., 2014; Nicotra & Garone, 2018) assume that a control law, stabilizing the system to an arbitrary equilibrium, is available a priori and enforce constraints by having the system track an adaptively changing virtual reference governor. A dynamic safety margin (DSM) (Nicotra & Garone, 2018) obtained from a safe level set of the prestabilized system's Lyapunov function is used to

regulate the governor motion. Recently, Arslan and Koditschek (2017) demonstrated safe navigation field tracking with a double integrator system, using the difference between the (squared) distance to locally sensed obstacles and the Lyapunov function to construct a DSM. Our prior work (Li, Arslan, & Atanasov, 2020) shows that directional trajectory bounds for a linear system may be used to construct a less conservative DSM, allowing fast and safe state tracking control in unknown environments. In contrast to prior reference governor works (Nicotra & Garone, 2018), this paper considers output tracking and provides an explicit construction of a governor-parameterized barrier function, which serves as a dynamic safety margin by measuring distances to the unsafe set. With the help of off-the-shelf simultaneous localization and mapping (Hornung, Wurm, Bennewitz, Stachniss, & Burgard, 2013) and geometric motion planning (LaValle, 2006) algorithms, our method can achieve safe navigation in unknown environments without requiring an a priori known navigation.

Contributions. The main contribution of this paper is a reference governor control design for *safe output tracking* subject to *locally sensed output constraints*. We introduce a *governor-parameterized barrier function* that compares the distance to constraint violation with the value of an output-regulation Lyapunov function. In contrast to existing literature, we handle output constraints that are known only at runtime. A PBF is constructed online using distance measurements in the system output space without complex optimization or preprocessing steps. We show that our PBF construction is a valid dynamic safety margin and prove safe and stable output tracking using a reference governor controller. Our algorithm achieves safe adaptive tracking for feedback-linearizable dynamical systems operating in unknown environments.

2. Problem statement

Consider a linear time-invariant dynamical system:

$$\dot{\mathbf{x}} = \mathbf{A}\mathbf{x} + \mathbf{B}\mathbf{u}, \quad \mathbf{x}(t_0) = \mathbf{x}_0,$$

 $\mathbf{y} = \mathbf{C}\mathbf{x},$ (1)

where $\mathbf{x} \in \mathbb{R}^n$ is the state, $\mathbf{u} \in \mathbb{R}^m$ is the control input, $\mathbf{y} \in \mathbb{R}^m$ is the output.

The goal of this paper is to design a controller such that the output \mathbf{y} of (1) tracks a reference path without violating safety constraints or adhering to pre-defined time scaling. To accommodate output constraints, we define an obstacle-free open set $\mathcal{F} \subset \mathbb{R}^m$ and a closed obstacle set $\mathcal{O} := \mathbb{R}^m \setminus \mathcal{F}$. Motivated by applications in autonomous system navigation, we assume that the obstacle set \mathcal{O} is not known a priori. Instead, the system can sense the distance from its output \mathbf{y} to \mathcal{O} only locally with a limited sensing range $\beta > 0$:

$$d_{s}(\mathbf{y}, \mathcal{O}) = \begin{cases} -\min\{d(\mathbf{y}, \partial \mathcal{O}), \beta\} & \text{if } \mathbf{y} \in \text{int}(\mathcal{O}) \\ \min\{d(\mathbf{y}, \partial \mathcal{O}), \beta\} & \text{if } \mathbf{y} \notin \text{int}(\mathcal{O}) \end{cases},$$
(2)

where $d(\mathbf{y}, \partial \mathcal{O}) := \min_{\mathbf{a} \in \partial \mathcal{O}} \|\mathbf{y} - \mathbf{a}\|$. We denote the interior of a set \mathcal{A} as $\operatorname{int}(\mathcal{A})$ and its closure as $\operatorname{cl}(\mathcal{A})$.

Problem 1. Let $\mathbf{r}:[0,1]\mapsto \mathcal{F}$ be a continuous function specifying an output reference path for the system in (1). Assume that $\mathbf{r}(0) = \mathbf{y}(t_0) \in \mathcal{F}$. Using local distance observations $d_s(\mathbf{y},\mathcal{O})$ of the obstacle set \mathcal{O} , design a control policy for (1) so that the output $\mathbf{y}(t)$ of the closed-loop system converges asymptotically to $\mathbf{r}(1)$, while remaining safe, i.e., $\mathbf{y}(t) \in \operatorname{cl}(\mathcal{F})$ for all $t \geq t_0$.

Remark 1. In robot navigation applications, a reference path **r** can be generated and updated online by continuously mapping the occupied space using distance observations (Hornung et al., 2013; Oleynikova, Taylor, Fehr, Siegwart, & Nieto, 2017) and replanning a path in free space using a motion planning algorithm (LaValle, 2006).

3. Setpoint control without constraints

We first discuss stabilizing the output of (1) to an arbitrary fixed point $\mathbf{g} \in \mathbb{R}^m$ without constraints.

Problem 2. Design a sufficiently smooth function $\mathbf{u} = \mathbf{k}(\mathbf{x}, \mathbf{g})$ such that for any constant $\mathbf{g} \in \mathbb{R}^m$, the closed-loop system:

$$\dot{\mathbf{x}} = \mathbf{A}\mathbf{x} + \mathbf{B}\,\mathbf{k}(\mathbf{x}, \mathbf{g}), \quad \mathbf{x}(t_0) = \mathbf{x}_0,
\mathbf{y} = \mathbf{C}\mathbf{x},$$
(3)

admits a **g**-parameterized equilibrium $\mathbf{x_g} = \mathbf{Xg}$ for some constant matrix $\mathbf{X} \in \mathbb{R}^{n \times m}$ and the output **y** converges to **g** exponentially.

Theorem 1 (*Francis* (1977)). Let $\mathbf{K} \in \mathbb{R}^{m \times n}$ be such that $(\mathbf{A} + \mathbf{B}\mathbf{K})$ is Hurwitz. If there exist matrices $\mathbf{X} \in \mathbb{R}^{n \times m}$ and $\mathbf{U} \in \mathbb{R}^{m \times n}$ that satisfy the regulator equations:

$$\mathbf{0} = \mathbf{AX} + \mathbf{BU},$$

$$\mathbf{0} = \mathbf{CX} - \mathbf{I},$$
(4)

then there exists a static state-feedback controller that solves Problem 2:

$$\mathbf{k}(\mathbf{x}, \mathbf{g}) = \mathbf{K}\mathbf{x} + (\mathbf{U} - \mathbf{K}\mathbf{X})\mathbf{g}. \tag{5}$$

Proof. Let $\bar{\mathbf{x}} := \mathbf{x} - \mathbf{Xg}$. Since \mathbf{X} and \mathbf{U} satisfy (4), the closed-loop system in (3) with $\mathbf{k}(\mathbf{x}, \mathbf{g})$ in (5) becomes:

$$\dot{\bar{\mathbf{x}}} = \mathbf{A}\mathbf{x} + \mathbf{B} [\mathbf{K}\mathbf{x} + (\mathbf{U} - \mathbf{K}\mathbf{X})\mathbf{g}]
= (\mathbf{A} + \mathbf{B}\mathbf{K})(\bar{\mathbf{x}} + \mathbf{X}\mathbf{g}) - (\mathbf{A} + \mathbf{B}\mathbf{K})\mathbf{X}\mathbf{g}
= (\mathbf{A} + \mathbf{B}\mathbf{K})\bar{\mathbf{x}},
\mathbf{y} = \mathbf{C}\bar{\mathbf{x}} + \mathbf{g}.$$
(6)

Since (A+BK) is Hurwitz by assumption, the closed-loop system in (6) is exponentially stable with equilibrium $\mathbf{x_g} = \mathbf{Xg}$ and steady-state output $\mathbf{y} = \mathbf{g}$. \square

Assumption 1. The pair (A, B) is stabilizable and

$$\operatorname{rank}\begin{bmatrix} \mathbf{A} & \mathbf{B} \\ \mathbf{C} & \mathbf{0} \end{bmatrix} = n + m \tag{7}$$

Under Assumption 1, the regulator equations (4) are guaranteed to have a solution (Huang, 2004, Theorem 1.9) and the static feedback controller in (5) solves Problem 2.

4. Safe output regulation via parametric barrier functions

Section 3 showed how to regulate the output of (1) under Assumption 1 to a desired reference point \mathbf{g} . Next, we consider Problem 2 in the presence of output constraints. We construct a \mathbf{g} -parameterized barrier function (PBF) that quantifies the trade-off between safety (distance from \mathbf{g} to the obstacle set \mathcal{O} in (2)) and the system energy. For controllable (\mathbf{A} , \mathbf{B}), following Theorem 1, the energy of (3) can be measured by a \mathbf{g} -parameterized quadratic Lyapunov function (Khalil, 2002):

$$V(\mathbf{x}; \mathbf{g}) = (\mathbf{x} - \mathbf{X}\mathbf{g})^{\mathsf{T}} \mathbf{P} (\mathbf{x} - \mathbf{X}\mathbf{g}), \qquad (8)$$

where \mathbf{P} is the unique solution of the Lyapunov equation $(\mathbf{A} + \mathbf{B}\mathbf{K})^{\top}\mathbf{P} + \mathbf{P}(\mathbf{A} + \mathbf{B}\mathbf{K}) = -\mathbf{Q}$ for any positive-definite symmetric matrix $\mathbf{Q} \in \mathbb{S}_{>0}^n$. The Lyapunov function can be expressed as $V(\mathbf{x};\mathbf{g}) = \|\mathbf{x} - \mathbf{X}\mathbf{g}\|_{\mathbf{P}}^2$ using a quadratic norm $\|\mathbf{x}\|_{\mathbf{P}} := \sqrt{\mathbf{x}^{\top}\mathbf{P}\mathbf{x}}$ on \mathbb{R}^n defined by $\mathbf{P} \in \mathbb{S}_{>0}^n$. The system output $\mathbf{y} = \mathbf{C}\mathbf{x}$ is Lipschitz continuous with respect to $\|\mathbf{x}\|_{\mathbf{P}}$, allowing us to relate the distance to the obstacle set \mathcal{O} with the distance to the desired equilibrium $\mathbf{x}_{\mathbf{g}} = \mathbf{X}\mathbf{g}$.

Lemma 1. For any $\mathbf{P} \in \mathbb{S}_{>0}^n$ with Cholesky factorization $\mathbf{P} = \mathbf{L}\mathbf{L}^{\top}$, there exists a global Lipschitz constant $L = \lambda_{\max}^{1/2}(\mathbf{L}^{-1}\mathbf{C}^{\top}\mathbf{C}\mathbf{L}^{-\top})$ such that:

$$\|\mathbf{C}\mathbf{x}_1 - \mathbf{C}\mathbf{x}_2\| \le L\|\mathbf{x}_1 - \mathbf{x}_2\|_{\mathbf{P}}, \ \forall \mathbf{x}_1, \mathbf{x}_2 \in \mathbb{R}^n.$$
 (9)

Proof. The result follows from the generalized Rayleigh quotient. $\hfill\Box$

Definition 1. Let $V(\mathbf{x}; \mathbf{g})$ be a **g**-parameterized Lyapunov function for output regulation to $\mathbf{g} \in \mathbb{R}^m$. Let $d_s(\mathbf{g}, \mathcal{O})$ be the truncated signed distance function to the obstacle set \mathcal{O} in (2). A **g**-parameterized barrier function (PBF) is:

$$b(\mathbf{x}; \mathbf{g}) := d_s^2(\mathbf{g}, \mathcal{O}) - L^2 V(\mathbf{x}; \mathbf{g})$$
(10)

where L is the Lipschitz constant in (9).

Proposition 1. Let $\mathbf{g} \in \mathcal{F}$. Consider the closed-loop system in (3) with controller in (5). The set $S(\mathbf{g}) := \{\mathbf{x} \mid b(\mathbf{x}; \mathbf{g}) \geq 0\}$ is positively invariant and the output $\mathbf{y}(t)$ converges to \mathbf{g} asymptotically without violating the output constraints, i.e., $\mathbf{y}(t) \in cl(\mathcal{F})$ for all $t \geq t_0$.

Proof. For fixed \mathbf{g} , the time derivative of $b(\mathbf{x}; \mathbf{g})$ is strictly positive, $\frac{\partial b}{\partial \mathbf{x}} \dot{\mathbf{x}} = -l^2 \frac{\partial V}{\partial \mathbf{x}} \dot{\mathbf{x}} > 0$, because $V(\mathbf{x}; \mathbf{g})$ is a Lyapunov function. Hence, $S(\mathbf{g})$ is forward invariant. Theorem 1 guarantees that $\mathbf{y}(t) \to \mathbf{g}$ and $\mathbf{x}(t) \to \mathbf{x}_{\mathbf{g}} = \mathbf{X}\mathbf{g}$. Finally, we show that, if $\mathbf{x}_0 \in S(\mathbf{g})$, then $\mathbf{y}(t) \in \operatorname{cl}(\mathcal{F})$ for all $t \geq t_0$. Since the time derivative of $b(\mathbf{x}; \mathbf{g})$ is positive, $b(\mathbf{x}(t); \mathbf{g}) \geq b(\mathbf{x}_0; \mathbf{g}) \geq 0$ for all $t \geq t_0$. From (4), (9) and (10):

$$b(\mathbf{x}(t); \mathbf{g}) \le d^{2}(\mathbf{g}, \partial \mathcal{O}) - L^{2} \|\mathbf{x}(t) - \mathbf{x}_{\mathbf{g}}\|_{\mathbf{p}}^{2}$$

$$< d^{2}(\mathbf{g}, \partial \mathcal{O}) - \|\mathbf{C}\mathbf{x}(t) - \mathbf{g}\|^{2}.$$
(11)

Hence, for all $t \geq t_0$, $\|\mathbf{y}(t) - \mathbf{g}\| \leq d(\mathbf{g}, \partial \mathcal{O})$, and since $\mathbf{g} \in \mathcal{F}$, $\mathbf{y}(t) \in \operatorname{cl}(\mathcal{F})$ for all $t \geq t_0$. \square

Remark 2. Proposition 1 and the remaining results in the paper hold when only a subspace of \mathbb{R}^m is constrained. Assume, without loss of generality, that only the first $m_1 \leq m$ dimensions are constrained so that $\mathcal{O} = \mathcal{O}_1 \times \mathcal{O}^{m-m_1}$, $\mathcal{F}_1 = \mathbb{R}^{m_1} \setminus \mathcal{O}_1$, and $\mathcal{F} = \mathcal{F}_1 \times \mathbb{R}^{m-m_1}$. The results can be extended by defining $d(\mathbf{y}, \partial \mathcal{O}) := \min_{\mathbf{b} \in \partial \mathcal{O}_1} \|\mathbf{b} - \mathbf{P}_1 \mathbf{y}\|$, where $\mathbf{P}_1 = [\mathbf{I}, \mathbf{0}] \in \mathbb{R}^{m_1 \times m}$ is a projection matrix. For example, noting that $\|\mathbf{P}_1 \mathbf{y} - \mathbf{P}_1 \mathbf{g}\| \leq \|\mathbf{y} - \mathbf{g}\|$, $\forall \mathbf{y}, \mathbf{g} \in \mathbb{R}^m$, (11) implies that

$$\min_{\mathbf{b} \in \partial \mathcal{O}_1} \|\mathbf{b} - \mathbf{P}_1 \mathbf{g}\| \ge \|\mathbf{P}_1 \mathbf{y}(t) - \mathbf{P}_1 \mathbf{g}\|,$$

i.e., $\mathbf{P}_1\mathbf{y}(t) \in \operatorname{cl}(\mathcal{F}_1)$, which means that $\mathbf{y}(t) \in \operatorname{cl}(\mathcal{F})$.

5. Safe adaptive output tracking using a reference governor

Section 4 discussed output regulation to a static reference point \mathbf{g} using a PBF to quantify safety. In this section, we develop an approach to adaptively change the regulation point $\mathbf{g}(t)$ so that the output of the closed-loop system in (3) tracks the desired path \mathbf{r} safely. Our control design consists of two parts: a virtual reference governor system whose state $\mathbf{g}(t)$ adaptively moves along the path \mathbf{r} and the closed-loop system in (3), tracking the time-varying reference point $\mathbf{X}\mathbf{g}(t)$. The structure of the reference-governor controller is visualized in Fig. 1.

Definition 2. A reference governor is a linear system:

$$\dot{\mathbf{g}} = -k_g \left(\mathbf{g} - \bar{\mathbf{g}} \right) \tag{12}$$

with gain $k_g > 0$, state $\mathbf{g} \in \mathbb{R}^m$, and input $\bar{\mathbf{g}} \in \mathbb{R}^m$.

We show that the slackness in the PBF safety metric in (10) can be used to move **g** along the reference path **r** without endangering safety or stability of the closed-loop system in (3).

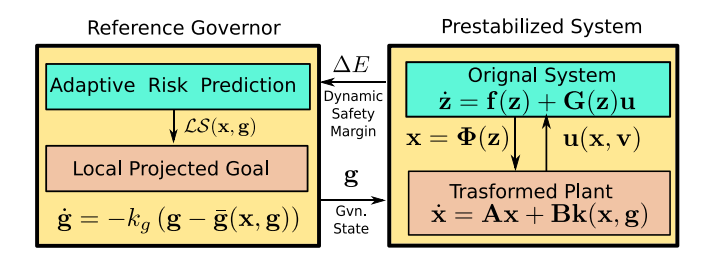


Fig. 1. Safe output tracking with a reference-governor controller: A virtual governor system with state \mathbf{g} adaptively tracks the desired reference path \mathbf{r} while ensuring that the output of a prestabilized system can track \mathbf{g} . A local safe zone $\mathcal{LS}(\mathbf{x},\mathbf{g})$ is constructed to determine the set of possible governor states that ensure safety and stability. A time-varying local goal $\mathbf{\bar{g}}$ is computed by projecting the reference path \mathbf{r} onto the boundary of $\mathcal{LS}(\mathbf{x},\mathbf{g})$. The governor system is controlled to track the local projected goal $\mathbf{\bar{g}}$ while sending its state \mathbf{g} to the controller, which is responsible to drive the system output asymptotically to \mathbf{g} .

Definition 3 (*Nicotra & Garone, 2018*). A continuous function $\Delta E(\mathbf{x}, \mathbf{g}) : \mathbb{R}^n \times \mathbb{R}^m \mapsto \mathbb{R}$ is a *dynamic safety margin* (DSM) for the closed-loop system in (3) if:

- 1. $\Delta E(\mathbf{x}, \mathbf{g}) \geq 0 \implies d_s(\mathbf{C}\mathbf{x}, \mathcal{O}) \geq 0$,
- 2. $\Delta E(\mathbf{x}_0, \mathbf{g}) = 0 \implies \Delta E(\mathbf{x}(t), \mathbf{g}) > 0, \forall t > t_0$
- 3. for all $\delta > 0$, there exists $\epsilon > 0$ such that $d_s(\mathbf{g}, \mathcal{O}) \geq \delta \implies \Delta E(\mathbf{x}_{\mathbf{g}}, \mathbf{g}) \geq \epsilon$.

A DSM is a measure of system safety, i.e., larger ΔE means that the system is safer with respect to the output constraints. The first condition requires that non-negative ΔE implies that the system is safe at the current moment, while the second condition requires certification of safety forward in time for fixed ${\bf g}$. The last condition requires that the DSM captures the slackness in the safety constraints.

Lemma 2. For $\mathbf{g} \in \mathcal{F}$, the \mathbf{g} -parameterized barrier function in (10) is a dynamic safety margin for the closed-loop system in (3): $\Delta E(\mathbf{x}, \mathbf{g}) = b(\mathbf{x}; \mathbf{g})$.

Proof. From (10), (8), (9), and (2):

$$\Delta E(\mathbf{x}, \mathbf{g}) \ge 0 \implies d_s^2(\mathbf{g}, \mathcal{O}) \ge L^2 \|\mathbf{x} - \mathbf{X}\mathbf{g}\|_{\mathbf{p}}^2$$

$$\implies d_s(\mathbf{g}, \mathcal{O}) \ge \|\mathbf{C}\mathbf{x} - \mathbf{g}\|$$

$$\implies d(\mathbf{g}, \partial \mathcal{O}) \ge \|\mathbf{C}\mathbf{x} - \mathbf{g}\|$$
(13)

Since $\mathbf{g} \in \mathcal{F}$ the last inequality implies that $\mathbf{y} = \mathbf{C}\mathbf{x} \in \operatorname{cl}(\mathcal{F})$ and, hence, $d_s(\mathbf{C}\mathbf{x}, \mathcal{O}) \geq 0$. The second requirement of Definition 3 follows from Proposition 1. The last one holds with $\epsilon = \min \left\{ \delta^2, \beta^2 \right\}$: $b(\mathbf{x}_{\mathbf{g}}; \mathbf{g}) = d_s^2(\mathbf{g}, \mathcal{O}) - 0 \geq \min \left\{ \delta^2, \beta^2 \right\} = \epsilon$. \square

In the rest of the paper, we study the case of a moving governor $\mathbf{g}(t)$. We denote the Lyapunov function and PBF by $V(\mathbf{x},\mathbf{g})$ and $b(\mathbf{x},\mathbf{g})$, instead of $V(\mathbf{x};\mathbf{g})$ and $b(\mathbf{x};\mathbf{g})$, to emphasize the fact that $\mathbf{g}(t)$ is time-varying. To guarantee safe output tracking, the input $\bar{\mathbf{g}}$ of the governor system in (12) must be chosen by jointly considering the geometry of the local safe space and the activeness of the prestabilized system. This trade-off is captured by the PBF $b(\mathbf{x},\mathbf{g})$. We define a set of feasible governor inputs that will not violate the safety or stability for the closed-loop system in (3).

Definition 4. A *local safe zone* is a time-varying set, determined by the joint system-governor state (\mathbf{x} , \mathbf{g}), a dynamic safety margin $\Delta E(\mathbf{x}, \mathbf{g})$, and a constant l > 1:

$$\mathcal{LS}(\mathbf{x}, \mathbf{g}) := \left\{ \mathbf{q} \in \mathbb{R}^m \mid \|\mathbf{q} - \mathbf{g}\|^2 \le l^{-1} \Delta E(\mathbf{x}, \mathbf{g}) \right\}. \tag{14}$$

Remark 3. The constant l > 1 in Definition 4 is needed to ensure that $\mathcal{LS}(\mathbf{x}, \mathbf{g}) \subset \mathcal{F}$. When $\Delta E(\mathbf{x}, \mathbf{g}) = 0$, $\mathcal{LS}(\mathbf{x}, \mathbf{g}) = \{\mathbf{g}\} \subset \mathcal{F}$. If $\Delta E(\mathbf{x}, \mathbf{g}) > 0$, then for any $\mathbf{q} \in \mathcal{LS}(\mathbf{x}, \mathbf{g})$, $\|\mathbf{q} - \mathbf{g}\|^2 < \Delta E(\mathbf{x}, \mathbf{g}) \leq d_s^2(\mathbf{g}, \mathcal{O})$, which implies that $\|\mathbf{q} - \mathbf{g}\| < d_s(\mathbf{g}, \mathcal{O})$, i.e., $\mathbf{q} \in \mathcal{F}$.

We show, in the proof of Theorem 2, that choosing $\bar{\mathbf{g}} \in \mathcal{LS}(\mathbf{x},\mathbf{g}) \subset \mathcal{F}$ ensures that system safety is guaranteed and the governor trajectory $\mathbf{g}(t)$ lies in \mathcal{F} and always eventually makes $\Delta E(\mathbf{x},\mathbf{g})$ strictly positive until reaching $\mathbf{r}(1)$. To make the governor progress along the reference path \mathbf{r} and lead the closed-loop system, we choose the governor input $\bar{\mathbf{g}}$ as the furthest point along \mathbf{r} that is contained in $\mathcal{LS}(\mathbf{x},\mathbf{g})$.

Definition 5. A local projected goal at system-governor state (\mathbf{x}, \mathbf{g}) is a point $\bar{\mathbf{g}} \in \mathcal{LS}(\mathbf{x}, \mathbf{g})$ that is furthest along the reference path \mathbf{r} :

$$\bar{\mathbf{g}} = \mathbf{r}(\bar{\sigma}), \quad \bar{\sigma} = \underset{\sigma \in [0,1]}{\operatorname{argmax}} \{ \sigma \mid \mathbf{r}(\sigma) \in \mathcal{LS}(\mathbf{x}, \mathbf{g}) \}.$$
 (15)

We summarize the closed-loop dynamics for the joint (\mathbf{x}, \mathbf{g}) system controlled by the output regulator in (5) and the reference-governor control law in (15):

$$\dot{\mathbf{x}} = (\mathbf{A} + \mathbf{B}\mathbf{K})(\mathbf{x} - \mathbf{X}\mathbf{g}),\tag{16a}$$

$$\dot{\mathbf{g}} = -k_g \left(\mathbf{g} - \bar{\mathbf{g}} \right), \tag{16b}$$

$$\mathbf{y} = \mathbf{C}\mathbf{x} \tag{16c}$$

Theorem 2. Given a reference path \mathbf{r} , consider the closed-loop system in (16). Suppose that the initial state $(\mathbf{x}_0, \mathbf{g}_0)$ satisfies:

$$\Delta E(\mathbf{x}_0, \mathbf{g}_0) > 0, \quad \mathbf{g}_0 = \mathbf{r}(0) = \mathbf{y}(t_0) \in \mathcal{F}, \tag{17}$$

where $\Delta E(\mathbf{x}, \mathbf{g})$ is the dynamic safety margin in (10). Then, the joint state (\mathbf{x}, \mathbf{g}) converges to $(\mathbf{Xr}(1), \mathbf{r}(1))$ without violating the output constraints, i.e., $\mathbf{y}(t) \in cl(\mathcal{F})$, $\forall t \geq t_0$.

Proof. The proof consists of three parts. First, we prove that the dynamics in (16) are updated continuously. Second, we show that the output constraints are not violated under (16). Last, we prove that the joint system (16) has a unique stable equilibrium point at $(\mathbf{Xr}(1), \mathbf{r}(1))$.

First, we show that the DSM $\Delta E(t) := b(\mathbf{x}(t), \mathbf{g}(t))$ is continuous. In Lemma 4, we prove that $\|\dot{\mathbf{g}}(t)\|$ is uniformly bounded by $k_g \beta \sqrt{l^{-1}}$ and therefore $\mathbf{g}(t)$ is continuous. Then, since the truncated signed distance function $d_s(\mathbf{g}(t), \mathcal{O})$ is continuous (Lemma 5) and $V(\mathbf{x}, \mathbf{g})$ is continuous in (\mathbf{x}, \mathbf{g}) , we show in Lemma 6 that $\Delta E(t)$ is also a continuous function in t. The state \mathbf{x} is regulated by a static feedback controller $\mathbf{k}(\mathbf{x}, \mathbf{g})$ and is also continuous. Hence, the system dynamics in (16) are updated continuously.

Second, we prove that safety is ensured, i.e., for all $t \geq t_0$, $\mathbf{y}(t) \in \operatorname{cl}(\mathcal{F})$, when $\mathbf{g}(t)$ is changing according to (16b). Lemma 8 shows that the set $\mathcal{S} := \{(\mathbf{x},\mathbf{g}) \in \mathbb{R}^n \times \mathbb{R}^m \mid \Delta E(\mathbf{x},\mathbf{g}) \geq 0\}$ is positively invariant for the closed-loop system in (16). Hence, $\Delta E(t) \geq 0$ for all $t \geq t_0$ and, by the first property of a dynamic safety margin in Definition 3, $d_s(\mathbf{y}(t),\mathcal{O}) \geq 0$ for all $t \geq t_0$. In detail, initially $\mathbf{g}_0 = \mathbf{y}_0 = \mathbf{r}(0) \in \mathcal{LS}(\mathbf{x}_0,\mathbf{g}_0)$ and $\Delta E(t_0) > 0$. The local projected goal $\bar{\mathbf{g}}$ in (15) is well defined and moves along the reference path \mathbf{r} , i.e., $\bar{\sigma}$ in (15) increases. As \mathbf{g} tracks $\bar{\mathbf{g}}$ using (16b), the system state \mathbf{x} tracks $\mathbf{X}\mathbf{g}$ using the controller in (5). During this process, the DSM $\Delta E(t) = b(\mathbf{x}(t),\mathbf{g}(t))$, as the difference of $d_s^2(\mathbf{g},\mathcal{O})$ and the scaled Lyapunov function V(t), is fluctuating and regulating the rate of change of \mathbf{g} (see Fig. 3). Lemma 7 shows that for $\bar{\mathbf{x}} = \mathbf{x} - \mathbf{X}\mathbf{g}$:

$$\dot{V}(t) \leq -\bar{\mathbf{x}}(t)^{\top} \mathbf{Q} \bar{\mathbf{x}}(t) + 2 \|\mathbf{X}^{\top} \mathbf{P} \bar{\mathbf{x}}(t) \| \|\dot{\mathbf{g}}(t) \|,
D_{+} \Delta E(t) \geq -2k_{g} M(t) \sqrt{\Delta E(t)/l} + L^{2} \bar{\mathbf{x}}(t)^{\top} \mathbf{Q} \bar{\mathbf{x}}(t),$$

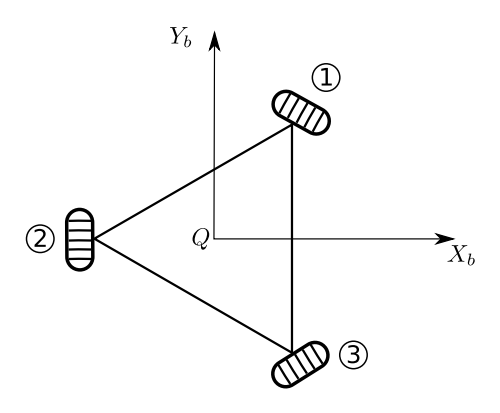


Fig. 2. A mobile robot with omnidirectional wheels.

where $D_+\Delta E(t)$ is the lower-right Dini derivative and M(t) is bounded pointwise in time. By continuity, $\Delta E(t)$ cannot become negative instantaneously without crossing 0 at some time $t=T_0$. Lemma 7 shows that $\Delta E(T_0+h)$ will bounce back from 0 to a strictly positive number after any such time T_0 .

Finally, we show that the joint state (\mathbf{x}, \mathbf{g}) converges to $(\mathbf{Xr}(1), \mathbf{r}(1))$ under the dynamics in (16). Note that $\mathbf{g}(t) \in \mathcal{LS}(\mathbf{x}(t), \mathbf{g}(t))$ and, from Remark 3, $\mathbf{g}(t) \in \mathcal{F}$ for all $t \geq t_0$. If $\mathbf{g} = \mathbf{r}(1)$, then $\mathbf{r}(1) \in \mathcal{LS}(\mathbf{x}, \mathbf{g})$, $\bar{\sigma} = 1$, and $\bar{\mathbf{g}} = \mathbf{r}(1)$ in (15). Then, $\dot{\mathbf{g}} \equiv 0$ and the output regulator in (5) drives \mathbf{x} to $\mathbf{Xr}(1)$. Hence, $(\mathbf{Xr}(1), \mathbf{r}(1))$ is an equilibrium point for (16). From Lemma 7, whenever $\Delta E(t) = 0$ at an arbitrary time $t = T_i$, it becomes strictly positive after some time h_i . Then, at $t_i = T_i + h_i$, the joint state $(\mathbf{x}(t_i), \mathbf{g}(t_i))$ satisfies:

$$\Delta E(t_i) > 0, \quad \mathbf{g}(t_i) \in \mathcal{F},$$
 (18)

and we are back to the case from the beginning. The local projected goal $\bar{\mathbf{g}}$ gets closer to $\mathbf{r}(1)$ and guides the joint system. It is not possible to have another equilibrium point because $\mathbf{g}(t) \in \mathcal{F}$ for all $t \geq t_0$ and, by the third DSM property in Definition 3, $\Delta E(\mathbf{Xg}, \mathbf{g}) \geq \epsilon$. From Definition 5, $\bar{\mathbf{g}}(t)$ can only stop moving at $\mathbf{r}(1)$ when $\Delta E(\mathbf{Xg}, \mathbf{g}) > 0$. Hence, the joint system in (16) has a unique stable equilibrium point at $(\mathbf{Xr}(1), \mathbf{r}(1))$.

In summary, Theorem 2 shows that the control law:

$$\pi(\mathbf{x}, \mathbf{g}) = \mathbf{k}(\mathbf{x}, \mathbf{g}),$$

$$\dot{\mathbf{g}} = -k_{g}(\mathbf{g} - \bar{\mathbf{g}}(\mathbf{x}, \mathbf{g})), \quad \mathbf{g}_{0} = \mathbf{y}(t_{0}) = \mathbf{r}(0),$$
(19)

combining the controller $\mathbf{k}(\mathbf{x}, \mathbf{g})$ in (5) and the reference governor in (12), (15) solves Problem 1 as long as the dynamic safety margin is strictly positive initially, $\Delta E(\mathbf{x}_0, \mathbf{g}_0) = b(\mathbf{x}_0, \mathbf{g}_0) > 0$.

6. Evaluation

This section evaluates our safe output-tracking controller on a simulated mobile robot, measuring distances to obstacles in an unknown environment.

System Model. Consider a mobile robot equipped three identical Swedish omnidirectional wheels (d'Andrea-Novel, Bastin, & Campion, 1992), shown in Fig. 2. Let m be the mass and I be the inertia around the Z_b axis (perpendicular to the X_b , Y_b plane in the body frame). The robot's motion is described by the position and orientation, (x, y, θ) , of the body frame and the positions of ϕ_1 , ϕ_2 , ϕ_3 of the three wheels. The robot's dynamics can be obtained using Euler–Lagrange equations subject to pure-rolling non-holonomic constraints for the three wheels (Campion

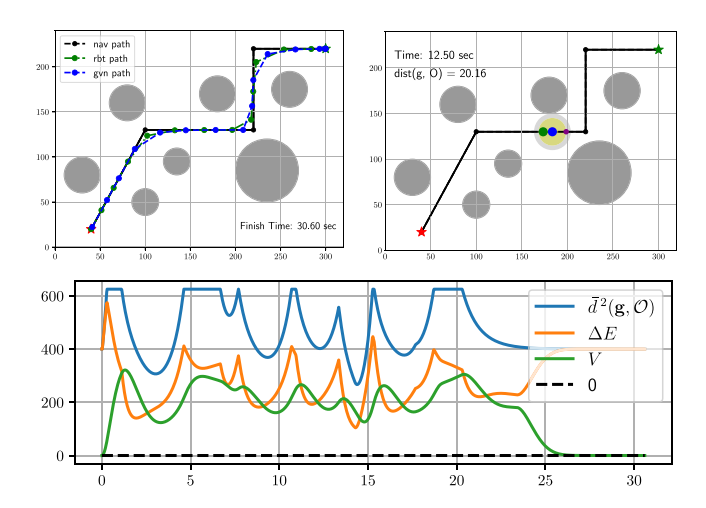


Fig. 3. Output-tracking control of an omnidirectional mobile robot navigating in an unknown environment with circular obstacles (gray). Top left shows the projection of the reference path ${\bf r}$ and the paths followed by the system and the governor. Top right shows a snapshot at time t=15 of the positions of system output ${\bf y}$ (green), governor state ${\bf g}$ (blue), local projected goal $\bar{{\bf g}}$ (purple), obstacle distance $\bar{d}({\bf g},\mathcal{O})$ (gray ball), and local safe zone \mathcal{LS} (yellow ball). The bottom plot shows the PBF $\Delta E({\bf x},{\bf g})=b({\bf x},{\bf g})$ (blue) and its safety $d_s^2({\bf g},\mathcal{O})$ (green) and stability $V({\bf x},{\bf g})$ (orange) components. The PBF never crosses the zero line, indicating that safe navigation is achieved. (For interpretation of the references to color in this figure legend, the reader is referred to the web version of this article.)

& Bastin, 1990; d'Andrea-Novel et al., 1992). When the non-holonomic constraints are considered, the wheel positions ϕ_i may be eliminated, leading to the following dynamics model:

$$\mathbf{M}_{1}\mathbf{R}^{\mathsf{T}}(\theta) \begin{bmatrix} \ddot{\mathbf{x}} \\ \ddot{\mathbf{y}} \\ \ddot{\theta} \end{bmatrix} = -\mathbf{J}_{1}^{\mathsf{T}}\mathbf{J}_{3}^{-1}\boldsymbol{\mu}, \tag{20}$$

with:

$$\mathbf{R}(\theta) = \begin{bmatrix} \cos(\theta) & -\sin(\theta) & 0 \\ \sin(\theta) & \cos(\theta) & 0 \\ 0 & 0 & 1 \end{bmatrix}, \quad \mathbf{J}_1 = \begin{bmatrix} -\frac{\sqrt{3}}{2} & \frac{1}{2} & d \\ 0 & -1 & d \\ \frac{\sqrt{3}}{2} & \frac{1}{2} & d \end{bmatrix},$$

$$\mathbf{M}_1 = \operatorname{diag}(m, m, I), \qquad \qquad \mathbf{J}_3 = \operatorname{diag}(r, r, r),$$

where d is the distance from the robot center to the wheels and r is the wheel radius. The input $\mu \in \mathbb{R}^3$ contains the generalized forces and torque.

We consider obstacles $\mathcal{O}_1 \subset \mathbb{R}^2$ with no constraints on orientation, i.e., $\mathcal{O} = \mathcal{O}_1 \times \{\emptyset\}$, as shown in Figs. 3 and 4. As mentioned in Remark 2, the distance $d(\mathbf{y}, \partial \mathcal{O})$ is defined as:

$$d(\mathbf{y}, \partial \mathcal{O}) = \min_{\mathbf{b} \in \partial \mathcal{O}_1} \|\mathbf{P}_1 \mathbf{y} - \mathbf{b}\|, \tag{21}$$

where $P_1 = [I, 0]$. An output reference path $\mathbf{r} : [0, 1] \mapsto \mathcal{F} \subset \mathbb{R}^3$ is provided as shown in Figs. 3 and 4 with desired orientation fixed at 0.

Environment Sensing and Path Generation. In an unknown environment, the obstacle set \mathcal{O}_1 is not known. In our simulations, a simulated Lidar sensor provides a set of points $\mathcal{P}(t) := \{\mathbf{p}_i(t)\}_i$ on the surface of the obstacle set \mathcal{O}_1 , depending on the (position) output $\mathbf{y}(t)$, with a maximum sensing range of $\beta=25$. The distance from the governor to the obstacle set is approximated as.

$$d(\mathbf{g}(t), \partial \mathcal{O}) \approx \min_{\mathbf{p} \in \mathcal{P}(t)} \|\mathbf{P}_1 \mathbf{g}(t) - \mathbf{p}\|. \tag{22}$$

Note that, the same Lidar hit points P(t) from output depth measurement are used in above expression. To obtain a feasible

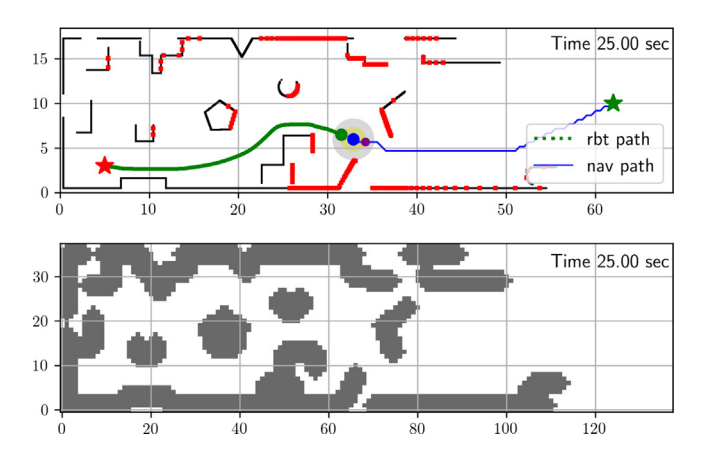


Fig. 4. Output-tracking control of an omnidirectional robot in an unknown environment with complex obstacles, sensed by a simulated Lidar. The Lidar provides distance measurements (red dots) from the robot position (green dot) to the obstacle set \mathcal{O}_1 (black surfaces). The reference path (blue curve) is recomputed online from the governor position (blue dot) to a goal location (green star). The local projected goal $\bar{\mathbf{g}}$ (purple dot) is computed based on the obstacle distance (gray ball) and the local safe zone (yellow ball). The bottom plot is the corresponding occupancy grid map at resolution 0.5 m/cell, where gray cells represent inflated obstacles (0.5 m inflation) and white cells represent free space. (For interpretation of the references to color in this figure legend, the reader is referred to the web version of this article.)

reference path \mathbf{r} , an occupancy grid (Hornung et al., 2013) is created and updated using the Lidar measurements (see Fig. 4). The grid map is discretized at resolution 0.5 m with a 0.5 m inflation around the obstacles. The unknown obstacle set \mathcal{O}_1 is over-approximated by the union $\hat{\mathcal{O}}_1(t)$ of all occupied cells up to time t. Using the latest map, the reference path \mathbf{r} is recomputed periodically using the A^* motion planner (LaValle, 2006). Since $\hat{\mathcal{O}}_1(t)$ is an over-approximation of \mathcal{O}_1 , the replanned reference paths lie within the free space \mathcal{F} . A snapshot of the occupancy grid map and one of the (re)planned paths (blue curves at top) are shown in Fig. 4.

Control Design. Observe that in Eq. (20), \mathbf{M}_1 , $\mathbf{R}(\theta)$, \mathbf{J}_1 , \mathbf{J}_3^{-1} are all invertible matrices. Hence, this model is feedback linearizable. Let $\mathbf{x} := [x, \dot{x}, y, \dot{y}, \theta, \dot{\theta}]^{\top} \in \mathbb{R}^6$ and $\mathbf{y} := [x, y, \theta]^{\top} \in \mathbb{R}^3$ be the new state and output vector. Applying control input:

$$\mu = \mathbf{J}_3 \mathbf{J}_1^{-\top} \mathbf{M}_1 \mathbf{R}^{\top}(\theta) \mathbf{u}, \tag{23}$$

transforms system (20) into a linear time-invariant form as in (1). Specifically, we have block-diagonal matrices $\mathbf{A} = \text{diag}(\mathbf{A}_1, \mathbf{A}_2, \mathbf{A}_3)$, $\mathbf{B} = \text{diag}(\mathbf{b}_1, \mathbf{b}_2, \mathbf{b}_3)$, $\mathbf{C} = \text{diag}(\mathbf{c}_1^\top, \mathbf{c}_2^\top, \mathbf{c}_3^\top)$ with elements $\mathbf{A}_i \in \mathbb{R}^{2 \times 2}$, $\mathbf{b}_i \in \mathbb{R}^2$;

$$\mathbf{A}_{i} = \begin{bmatrix} 0 & 1 \\ 0 & 0 \end{bmatrix}, \qquad \mathbf{b}_{i} = \begin{bmatrix} 0 \\ 1 \end{bmatrix}, \qquad \mathbf{c}_{i} = \begin{bmatrix} 1 \\ 0 \end{bmatrix}, \tag{24}$$

for i = 1, 2, 3. It can be verified that Assumption 1 is satisfied, and the regulator equation (4) is solved by $\mathbf{X} = \mathbf{C}^{\top}$ and $\mathbf{U} = \mathbf{0}$.

With $\bar{\mathbf{x}} = (\mathbf{x} - \mathbf{C}^{\top} \mathbf{g})$, the state-feedback controller $\mathbf{k}(\mathbf{x}, \mathbf{g}) = \mathbf{K}\bar{\mathbf{x}}$, with $\mathbf{K} = -\mathbf{I} \otimes [2.553, 1.9478]$, can drive the system output to an arbitrary reference \mathbf{g} . To define the PBF $\Delta E(\mathbf{x}, \mathbf{g}) = b(\mathbf{x}, \mathbf{g})$ in (10), we choose a quadratic Lyapunov function $V(\mathbf{x}, \mathbf{g}) = \bar{\mathbf{x}}^{\top} \mathbf{P} \bar{\mathbf{x}}$ with:

$$\mathbf{P} = \mathbf{I} \otimes \begin{bmatrix} 1.7508, & 0.7769 \\ 0.7769, & 0.9739 \end{bmatrix} \in \mathbb{S}_{>0}^{6}, \tag{25}$$

Lipschitz constant $L \approx 0.9403$, computed using Lemma 1, and sensing range $\beta = 25$. The governor control law in (12), (14), (15) is defined with l = 1.001 and $k_{\rm g} = 1.0$.

Simulation results. Fig. 3 shows the behavior of the closed-loop joint system in a constrained output tracking simulation.

Our control policy (19) successfully enforces the locally sensed obstacle avoidance constraints and drives the system to the goal configuration $\mathbf{r}(1)$. During this process, $\Delta E(t)$ is determined by the difference in the size of the local free space and the value of the Lyapunov function V(t) as shown in the bottom plot. The governor is controlled adaptively based on $\Delta E(t)$, slowing down when $\Delta E(t)$ is small and speeding up when it is large. In Fig. 4, we test our controller in a more challenging environment with nonconvex obstacles. With the same controller parameters described above, the system reaches the goal without collisions.

7. Conclusion

This paper developed an output-tracking controller that provides formal safety and stability guarantees for feedbacklinearizable control-affine nonlinear systems. We showed that reference-governor techniques can be extended to output tracking with distance measurements to an unsafe set. A key component of our design was a governor-parameterized barrier function, which uses the trade-off between the safe distance and the system Lyapunov function to define a local safe set for the system and governor states. The slackness in the safe set allows the governor to track the reference and the system to track the governor without endangering safety or stability. Our approach allows safe autonomous navigation in a priori unknown unstructured environments. The simple structure of the safety conditions in our design offers a promising research avenue for safe control with learned and approximate system dynamics and constraints.

Appendix

Lemma 3 (*Fitzpatrick, 1980*). Let (\mathcal{X}, μ) be a metric space and let $\mathcal{A} \subseteq \mathcal{X}$ be nonempty. The point-to-set distance function $d(\cdot, \mathcal{A})$: $\mathcal{X} \mapsto \mathbb{R}$ defined by $d(\cdot, \mathcal{A}) := \inf\{\mu(\mathbf{x}, \mathbf{a}) \mid \mathbf{a} \in \mathcal{A}\}$ is 1-Lipschitz:

$$|\textit{d}(\mathbf{x},\mathcal{A}) - \textit{d}(\mathbf{y},\mathcal{A})| \leq \mu(\mathbf{x},\mathbf{y}), \quad \forall \mathbf{x},\mathbf{y} \in \mathcal{X},$$

and, hence, uniformly continuous.

Lemma 4. The rate of change of the governor state in (12) is uniformly bounded by a constant, $\|\dot{\mathbf{g}}(t)\| \leq k_g \beta \sqrt{l^{-1}}$, and $\mathbf{g}(t)$ is continuous.

Proof. Considering (12), Definition 5, and 4:

$$\|\dot{\mathbf{g}}(t)\| = k_g \|\mathbf{g}(t) - \bar{\mathbf{g}}(t)\| \le k_g \sqrt{\Delta E(t)/l}.$$
(A.1)

With $\Delta E(\mathbf{x}, \mathbf{g}) = b(\mathbf{x}, \mathbf{g})$, from Definition 1 and (2), we know that $\Delta E(\mathbf{x}, \mathbf{g}) \leq d_s^2(\mathbf{g}(t), \mathcal{O}) \leq \beta^2$. Hence, $\|\dot{\mathbf{g}}(t)\| \leq k_g \beta \sqrt{l^{-1}}$ and $\mathbf{g}(t)$ is continuous (Filippov, 1988). \square

Lemma 5. The function $d_s(\mathbf{g}(t), \mathcal{O})$ is continuous when $\mathbf{g}(t) \in \mathcal{F}$.

Proof. When $\mathbf{g}(t) \in \mathcal{F}$, from definition (2), we have $d_s(\mathbf{g}(t), \mathcal{O}) = \min \{d(\mathbf{g}(t), \partial \mathcal{O}), \beta\}$. The min operation is continuous, $d(\mathbf{g}(t), \partial \mathcal{O})$ is continuous because $\mathbf{g}(t)$ is continuous by Lemma 4 and $d(\cdot, \partial \mathcal{O})$ is continuous by Lemma 3. \square

Lemma 6. The Lyapunov function $V(t) = V(\mathbf{x}(t), \mathbf{g}(t))$ in (8) and the dynamic safety margin $\Delta E(t) = b(\mathbf{x}(t), \mathbf{g}(t))$ in (10) are continuous functions in time.

Proof. From Lemma 4, we know that $\mathbf{g}(t)$ is continuous. Because $V(\mathbf{x}, \mathbf{g})$ is continuous in \mathbf{x} , \mathbf{g} , we have $V(t) = V(\mathbf{x}(t), \mathbf{g}(t))$ continuous in time. By Lemma 5, $d_s(\mathbf{g}(t), \mathcal{O})$ is continuous in time and, hence, $\Delta E(t) = d_s^2(\mathbf{g}(t), \mathcal{O}) - L^2V(t)$ is continuous in time. \square

Lemma 7. For $\Delta E(t) = b(\mathbf{x}(t), \mathbf{g}(t))$ defined in (10), let $T_0 \geq t_0$ be such that $\Delta E(T_0) = 0$. Then, the lower-right Dini derivative of $\Delta F(t)$.

$$D_{+}\Delta E(t) := \liminf_{h \to 0^{+}} \frac{\Delta E(t+h) - \Delta E(t)}{h}$$
(A.2)

satisfies $D_+\Delta E(T_0) > 0$ and there exists h > 0, such that $\Delta E(T_0 + h) > 0$.

Proof. Note that $\Delta E(t)$ is not differentiable everywhere due to the truncated signed distance function $d_s(\mathbf{g}(t), \mathcal{O})$ in its definition. We use the lower-right Dini derivative $D_+\Delta E(t)$ instead. Let $\hat{d}(t,h) := \max\{d_s(\mathbf{g}(t), \mathcal{O}), d_s(\mathbf{g}(t+h), \mathcal{O})\}$. From Lemma 3:

$$d_s(\mathbf{g}(t+h), \mathcal{O}) - d_s(\mathbf{g}(t), \mathcal{O}) \ge -\|\mathbf{g}(t) - \mathbf{g}(t+h)\|.$$

Hence, $\Delta E(t+h) - \Delta E(t) \ge -2\|\mathbf{g}(t) - \mathbf{g}(t+h)\|\hat{d}(t,h) + L^2(V(t) - V(t+h))$ and

$$D_{+}\Delta E(t) \ge -2\|\dot{\mathbf{g}}(t)\|d_{s}(\mathbf{g}(t),\mathcal{O}) - L^{2}\dot{V}(t) \tag{A.3}$$

From (8), with $\bar{\mathbf{x}} = \mathbf{x} - \mathbf{X}\mathbf{g}$:

$$\dot{V}(t) = 2\bar{\mathbf{x}}^{\mathsf{T}} \mathbf{P} \left((\mathbf{A} + \mathbf{B} \mathbf{K}) \bar{\mathbf{x}} - \mathbf{X} \dot{\mathbf{g}} \right)
= -\bar{\mathbf{x}}^{\mathsf{T}} \mathbf{Q} \bar{\mathbf{x}} - 2\bar{\mathbf{x}}^{\mathsf{T}} \mathbf{P} \mathbf{X} \dot{\mathbf{g}}
\leq -\bar{\mathbf{x}}^{\mathsf{T}} \mathbf{Q} \bar{\mathbf{x}} + 2 \|\mathbf{X}^{\mathsf{T}} \mathbf{P} \bar{\mathbf{x}}\| \|\dot{\mathbf{g}}\|.$$
(A.4)

From Lemma 4, $\|\dot{\mathbf{g}}(t)\| \le k_g \sqrt{\Delta E(t)/l}$, and therefore:

$$D_{+}\Delta E(t) \ge -2M(t)\|\dot{\mathbf{g}}(t)\| + L^{2}\bar{\mathbf{x}}(t)^{\top}\mathbf{Q}\bar{\mathbf{x}}(t)$$

$$\ge -2k_{g}M(t)\sqrt{\Delta E(t)/l} + L^{2}\bar{\mathbf{x}}(t)^{\top}\mathbf{Q}\bar{\mathbf{x}}(t)$$
(A.5)

where $M(t) = \bar{d}(\mathbf{g}(t), \mathcal{O}) + L^2 \|\mathbf{X}^{\top} \mathbf{P} \bar{\mathbf{x}}(t)\| \leq \beta + L^2 \|\mathbf{X}\| \|\mathbf{P}\| \|\bar{\mathbf{x}}(t)\| < \infty$ for bounded $\|\bar{\mathbf{x}}(t)\|$. From (10),

$$\lambda_{\min}(\mathbf{P})\|\bar{\mathbf{x}}(t)\|^2 \le V(t) \le \frac{\beta^2 - \Delta E(t)}{t^2},\tag{A.6}$$

which implies $\|\bar{\mathbf{x}}\|$ and M(t) are bounded, for $t=T_0$ such that $\Delta E(T_0)=0$.

Note that $\mathbf{g}(t) \in \mathcal{LS}(\mathbf{x}(t), \mathbf{g}(t)) \subset \mathcal{F}$, so $\Delta E(t) > 0$ when $V(t) = \bar{\mathbf{x}}(t)^{\mathsf{T}} \mathbf{P} \bar{\mathbf{x}}(t) = 0$. Therefore, $\Delta E(t) = 0$ and $\bar{\mathbf{x}}(t) = 0$ cannot happen simultaneously. Plugging $t = T_0$ such that $\Delta E(T_0) = 0$ into (A.5),

$$D_{+}\Delta E(T_{0}) \geq L^{2}\bar{\mathbf{x}}(T_{0})^{\top}\mathbf{Q}\bar{\mathbf{x}}(T_{0}) > 0 \tag{A.7}$$

since $\bar{\mathbf{x}}(T_0) \neq 0$, $\mathbf{Q} \in \mathbb{S}_{>0}^n$, and L > 0. Let $\dot{\gamma} \equiv 0$ with initial condition $\gamma(T_0) = 0$. By the Comparison Lemma (Khalil, 2002), $\Delta E(T_0 + h) > \gamma(T_0 + h) = 0$ for some h > 0. \square

Lemma 8. Consider the closed-loop system in (16). Then, the set $S := \{(\mathbf{x}, \mathbf{g}) \in \mathbb{R}^n \times \mathbb{R}^m \mid \Delta E(\mathbf{x}, \mathbf{g}) \geq 0\}$ is positively invariant.

Proof. By inequality (A.7), S is forward invariant if and only if the vector field defining the joint (\mathbf{x}, \mathbf{g}) system in (16) belongs to the Bouligand tangent cone of S for all $(\mathbf{x}, \mathbf{g}) \in S$. The tangent cone is trivial except on the boundary of S (see Blanchini & Miani, 2008) so the condition needs to be checked only for $(\mathbf{x}, \mathbf{g}) \in \partial S$. Since S is defined implicitly by the function $\Delta E(\mathbf{x}, \mathbf{g})$, the tangent cone is equal to the hypograph of the lower-right derivative of $\Delta E(\mathbf{x}, \mathbf{g})$ (Aubin, 1999, Prop. 3.3.2). In other words, S is forward invariant if and only if for all t such that $\Delta E(t) := \Delta E(\mathbf{x}(t), \mathbf{g}(t)) = 0$, we have $D_+\Delta E(t) \geq 0$, where $D_+\Delta E(t)$ is the lower-right Dini derivative of $\Delta E(t)$ evaluated along the flow of (16). This is concluded in Lemma 7.

References

Abel, I., Janković, M., & Krstić, M. (2020). Constrained control of input delayed systems with partially compensated input delays. In *Dynamic systems and* control conference.

Ames, A. D., Coogan, S., Egerstedt, M., Notomista, G., Sreenath, K., & Tabuada, P. (2019). Control barrier functions: Theory and applications. In *IEEE European control conference* (pp. 3420–3431).

Ames, A. D., Galloway, K., Sreenath, K., & Grizzle, J. W. (2014). Rapidly exponentially stabilizing control Lyapunov functions and hybrid zero dynamics. *IEEE Transactions on Automatic Control (TAC)*, 59(4), 876–891.

Ames, A. D., Grizzle, J. W., & Tabuada, P. (2014). Control barrier function based quadratic programs with application to adaptive cruise control. In *IEEE conference on decision and control* (pp. 6271–6278).

Ames, A. D., Xu, X., Grizzle, J. W., & Tabuada, P. (2017). Control barrier function based quadratic programs for safety critical systems. *IEEE Transactions on Automatic Control (TAC)*, 62(8), 3861–3876.

Arslan, O., & Koditschek, D. E. (2017). Smooth extensions of feedback motion planners via reference governors. In *IEEE international conference on robotics* and automation.

Aubin, J.-P. (1999). The method of characteristics revisited. A viability approach. arXiv preprint: Math/9906178.

Bansal, S., Chen, M., Herbert, S., & Tomlin, C. J. (2017). Hamilton-Jacobi reachability: A brief overview and recent advances. In *IEEE conference on decision and control* (pp. 2242–2253).

Barry, A. J., Majumdar, A., & Tedrake, R. (2012). Safety verification of reactive controllers for UAV flight in cluttered environments using barrier certificates. In *IEEE international conference on robotics and automation* (pp. 484–490).

Bemporad, A. (1998). Reference governor for constrained nonlinear systems. *IEEE Transactions on Automatic Control (TAC)*, 43(3), 415–419.

Blanchini, F., & Miani, S. (2008). Set-theoretic methods in control. Vol. 78. Springer. Borrelli, F., Bemporad, A., & Morari, M. (2017). Predictive control for linear and hybrid systems. Cambridge University Press.

Borrmann, U., Wang, L., Ames, A. D., & Egerstedt, M. (2015). Control barrier certificates for safe swarm behavior. *IFAC-PapersOnLine*, 68–73.

Bravo, J. M., Alamo, T., & Camacho, E. F. (2006). Robust MPC of constrained discrete-time nonlinear systems based on approximated reachable sets. *Automatica*, 42(10), 1745–1751.

Breeden, J., & Panagou, D. (2021). High relative degree control barrier functions under input constraints. In *IEEE conference on decision and control* (pp. 6119–6124).

Burridge, R., Rizzi, A., & Koditschek, D. (1999). Sequential composition of dynamically dexterous robot behaviors. *The International Journal of Robotics Research (IJRR)*, 18(6), 534–555.

Campion, G., & Bastin, G. (1990). On adaptive linearizing control of omnidirectional mobile robots. In *Robust control of linear systems and nonlinear control* (pp. 531–538). Springer.

Chen, M., Herbert, S., & Tomlin, C. J. (2017). Exact and efficient Hamilton-Jacobi guaranteed safety analysis via system decomposition. In *IEEE international conference on robotics and automation* (pp. 87–92).

Choi, J. J., Lee, D., Sreenath, K., Tomlin, C. J., & Herbert, S. L. (2021). Robust control barrier-value functions for safety-critical control. In *IEEE conference on decision and control* (pp. 6814–6821). IEEE.

Cosner, R. K., Singletary, A. W., Taylor, A. J., Molnar, T. G., Bouman, K. L., & Ames, A. D. (2021). Measurement-robust control barrier functions: Certainty in safety with uncertainty in state. In *International conference on intelligent robots and systems* (pp. 6286–6291). IEEE.

d'Andrea-Novel, B., Bastin, G., & Campion, G. (1992). Dynamic feedback linearization of nonholonomic wheeled mobile robots. In *IEEE international conference on robotics and automation* (pp. 2527–2528).

Filippov, A. F. (1988). Differential equations with discontinuous righthand sides: control systems. Vol. 18. Springer Science & Business Media.

Fisac, J. F., Chen, M., Tomlin, C. J., & Sastry, S. S. (2015). Reach-avoid problems with time-varying dynamics, targets and constraints. In *International* conference on hybrid systems: computation and control (pp. 11–20).

Fitzpatrick, S. (1980). Metric projections and the differentiability of distance functions. *Bulletin of Australian Mathematical Society*, 22(2), 291–312. http://dx.doi.org/10.1017/S0004972700006596.

Francis, B. A. (1977). The linear multivariable regulator problem. SIAM Journal on Control and Optimization, 15(3), 486-505.

Gao, Y., Gray, A., Tseng, H. E., & Borrelli, F. (2014). A tube-based robust nonlinear predictive control approach to semiautonomous ground vehicles. *Vehicle System Dynamics*, 52(6), 802–823.

Gao, F., Wu, W., Lin, Y., & Shen, S. (2018). Online safe trajectory generation for quadrotors using fast marching method and bernstein basis polynomial. In IEEE international conference on robotics and automation (pp. 344–351).

Grüne, L., & Pannek, J. (2017). Nonlinear model predictive control. Springer.

Herbert, S. L., Chen, M., Han, S., Bansal, S., Fisac, J. F., & Tomlin, C. J. (2017). FaS-Track: A modular framework for fast and guaranteed safe motion planning. In *IEEE conference on decision and control* (pp. 1517–1522). Hornung, A., Wurm, K. M., Bennewitz, M., Stachniss, C., & Burgard, W. (2013). OctoMap: An efficient probabilistic 3D mapping framework based on octrees. *Autonomous Robots*, 34(3), 189–206.

- Huang, J. (2004). Nonlinear output regulation: Theory and applications. SIAM.
- Jankovic, M. (2018). Robust control barrier functions for constrained stabilization of nonlinear systems. Automatica, 96, 359–367.
- Khalil, H. (2002). Nonlinear systems. Prentice Hall.
- Kolmanovsky, I., Garone, E., & Di Cairano, S. (2014). Reference and command governors: A tutorial on their theory and automotive applications. In *IEEE American control conference* (pp. 226–241).
- Kousik, S., Vaskov, S., Bu, F., Johnson-Roberson, M., & Vasudevan, R. (2020). Bridging the gap between safety and real-time performance in receding-horizon trajectory design for mobile robots. The International Journal of Robotics Research (IJRR).
- LaValle, S. (2006). Planning algorithms. Cambridge University Press.
- Li, Z., Arslan, O., & Atanasov, N. (2020). Fast and safe path-following control using a state-dependent directional metric. In *IEEE international conference on robotics and automation*.
- Long, K., Qian, C., Cortés, J., & Atanasov, N. (2021). Learning barrier functions with memory for robust safe navigation. *IEEE Robotics and Automation Letters* (*RA-L*), 6(3), 4931–4938.
- Majumdar, A., & Tedrake, R. (2017). Funnel libraries for real-time robust feedback motion planning. The International Journal of Robotics Research (IJRR), 36(8), 947–982.
- Mayne, D. Q., Rawlings, J. B., Rao, C. V., & Scokaert, P. O. (2000). Constrained model predictive control: Stability and optimality. *Automatica*, 36(6), 789–814.
- Nguyen, Q., & Sreenath, K. (2016). Exponential control barrier functions for enforcing high relative-degree safety-critical constraints. In *IEEE American* control conference (pp. 322–328).
- Nicotra, M. M., & Garone, E. (2018). The explicit reference governor: A general framework for the closed-form control of constrained nonlinear systems. *IEEE Control Systems Magazine*, 38(4), 89–107.
- Oleynikova, H., Taylor, Z., Fehr, M., Siegwart, R., & Nieto, J. (2017). Voxblox: Incremental 3D euclidean signed distance fields for on-board MAV planning. In IEEE/RSJ international conference on intelligent robots and systems.
- Ong, P., & Cortés, J. (2019). Universal formula for smooth safe stabilization. In *IEEE conference on decision and control* (pp. 2373–2378).
- Santillo, M., & Jankovic, M. (2021). Collision free navigation with interacting, noncommunicating obstacles. In *American control conference* (pp. 1637–1643). IFFF
- Sontag, E. D. (1983). A Lyapunov-like characterization of asymptotic controllability. SIAM Journal on Control and Optimization, 21(3), 462–471.

- Sontag, E. D. (1989). A 'universal' construction of Artstein's theorem on nonlinear stabilization. *Systems & Control Letters*, 13(2), 117–123.
- Tedrake, R., Manchester, I. R., Tobenkin, M., & Roberts, J. W. (2009). LQR-trees: Feedback motion planning via sums-of-squares verification. *The International Journal of Robotics Research (IJRR)*.
- Wu, G., & Sreenath, K. (2016). Safety-critical control of a planar quadrotor. In *American control conference* (pp. 2252–2258).
- Xiao, W., & Belta, C. (2019). Control barrier functions for systems with high relative degree. In *IEEE conference on decision and control* (pp. 474–479).
- Xu, X. (2018). Constrained control of input-output linearizable systems using control sharing barrier functions. Automatica, 87, 195–201.



Zhichao Li is a Ph.D. student in Electrical and Computer Engineering at the University of California San Diego, La Jolla, CA, USA. He received a B. Eng. degree from the School of Astronautics, Northwestern Polytechnical University, Xi'an, Shaanxi, China in 2013 and an M.S. degree in Electrical Engineering from the School of Electrical, Computer and Energy Engineering, Arizona State University, Tempe, AZ, in 2016. His research interests include control theory and motion planning with applications to mobile robotics.



Nikolay Atanasov is an Assistant Professor of Electrical and Computer Engineering at the University of California San Diego, La Jolla, CA, USA. He obtained a B.S. degree in Electrical Engineering from Trinity College, Hartford, CT, USA in 2008, and M.S. and Ph.D. degrees in Electrical and Systems Engineering from University of Pennsylvania, Philadelphia, PA, USA in 2012 and 2015, respectively. His research focuses on robotics, control theory, and machine learning with applications to active perception problems for autonomous mobile robots. He works on probabilistic models that unify

geometric and semantic information in simultaneous localization and mapping (SLAM) and on optimal control and reinforcement learning algorithms for minimizing uncertainty in probabilistic models. Dr. Atanasov's work has been recognized by the Joseph and Rosaline Wolf award for the best Ph.D. dissertation in Electrical and Systems Engineering at the University of Pennsylvania in 2015, the best conference paper award at the IEEE International Conference on Robotics and Automation (ICRA) in 2017, and the NSF CAREER award in 2021.